Global Protein-Turnover Quantification in *Escherichia coli* Reveals Cytoplasmic Recycling under Nitrogen-Limitation

Meera Gupta[1,2,3,*], Alex Johnson[1,2,3,*], Edward Cruz[2,3], Eli Costa[2], Randi Guest[3], Sophia Hsin-Jung Li[3], Elizabeth M Hart[3,4], Thao Nguyen[1,2,3], Michael Stadlmeier[2,3], Benjamin P. Bratton[2,3,5,6], Thomas J. Silhavy[3], Ned S. Wingreen[2,3], Zemer Gitai[3], Martin Wühr[1,2,3,#]

1 Department of Chemical and Biological Engineering, Princeton University, Princeton, NJ
2 Lewis-Sigler Institute for Integrative Genomics, Princeton University, Princeton, NJ
3 Department of Molecular Biology, Princeton University, Princeton, NJ
4 Department of Microbiology, Harvard Medical School, Boston, MA
5 Vanderbilt Institute of Infection, Immunology, and Inflammation, Nashville, TN
6 Department of Pathology, Microbiology, and Immunology, Vanderbilt University Medical Center, Nashville, TN

* Equally contributed
#Correspondence: wuhr@princeton.edu

Summary

Protein turnover is a critical regulatory mechanism for proteostasis. However, proteome-wide turnover quantification is technically challenging and, even in the well-studied *E. coli* model, reliable measurements remain scarce.
Here, we quantify the degradation of ~3.2k *E. coli* proteins under 12 conditions by combining heavy isotope labeling with complement reporter ion quantification and find that cytoplasmic proteins are recycled when nitrogen is limited. Furthermore, we show that protein degradation rates are generally independent of cell division rates, and we used knockout experiments to assign substrates to the known ATP-dependent proteases. Surprisingly, we find that none are responsible for the observed cytoplasmic protein degradation in nitrogen limitation, suggesting that a major proteolysis pathway in *E. coli* remains to be discovered. Thus, we introduce broadly applicable technology for protein turnover measurements. We provide a rich resource for protein half-lives and protease substrates in *E. coli,* complementary to genomics data, that will allow researchers to decipher the control of proteostasis.

Introduction

Protein degradation is central to protein homeostasis (proteostasis) and is critical in most cellular pathways (Cohen-Kaplan et al., 2016; Mahmoud and Chien, 2018). As environments change, modification of degradation rates can rapidly adapt protein abundances to desired levels. Even if protein levels are modulated via transcription or translation, a protein's response time is set by its replacement rate (Alon, 2006; Rosenfeld and Alon, 2003). Unsurprisingly, many signaling and transcriptional regulatory proteins exhibit short half-lives (Auld and Silver, 2006; Liu et al., 2012; Pahl and Baeuerle, 1996; Wettstadt and Llamas, 2020). Protein degradation is important in health and disease, for example in cancer and neurodegenerative disorders (Jang, 2018; Labbadia and Morimoto, 2015). Additionally, protein degradation plays an important metabolic role. It has been shown that bacteria and yeast cells increase their proteome turnover rates under starvation conditions, presumably generating and recycling scarce amino acids (Borek et al., 1958; Halvorson, 1958; Kuroda et al., 2001; Mandelstam, 1957).

Quantitative models have been developed to describe the dependence of global protein expression on cells' physiological characteristics, most notably cell doubling times. These models are probably the most well-developed in the model bacterium *E. coli* (Erickson et al., 2017; Klumpp et al., 2009). The cell cycle time in *E. coli* varies from 20 minutes in rich media to the cessation of division under starvation. Transcription rates typically increase with cell division rates, while translation rates remain constant (Liang et al., 1999; Liang et al., 2000). Knowing how global parameters scale with physiological cell states allows for remarkable quantitative predictions for gene expression changes across different growth conditions (Erickson *et al.*, 2017; Klumpp *et al.*, 2009). However, active protein degradation is typically ignored in these models. Instead, proteins are assumed to be completely stable and only diluted via cell growth and division. This simplification is likely due to a lack of reliable genome-wide degradation rate measurements under varying growth conditions. It is still unclear how active degradation rates scale with changing cell cycle times and how this affects global gene expression regulation. Presumably due to the lack of reliable genome-wide turnover resources, most systems biology studies have ignored the contribution of protein degradation rates in modeling protein homeostasis or dynamics (Balakrishnan et al., 2021; Belliveau et al., 2021; Scott et al., 2010). Knowledge of protein degradation rates and how they scale with the physiological characteristics of cells would improve predictive models of protein expression across various cell states.

Even for the proteins we know to be degraded, it is often unclear how these proteins are marked for destruction and which protease is responsible. Cells have developed sophisticated mechanisms to recognize and degrade specific proteins. In bacteria, selective proteolysis is executed by ATP-dependent proteases (Mahmoud and Chien, 2018). While many proteases can digest unfolded proteins and peptides, unfolding a protein for degradation requires energy. In *E. coli*, four ATP-dependent proteases are known: ClpP, Lon, HslV, and FtsH. Pulldown experiments with proteolytic-dead mutants or protein-array studies have allowed the proteome-wide identification of putative substrates (Arends et al., 2018; Flynn et al., 2003; Tsai et al., 2017; Westphal et al., 2012). Orthogonally, individual substrates have been assigned to the four proteases by measuring the degradation of individual proteins in protease knockout strains or via *in vitro* assays (Camberg et al., 2009; Schweder et al., 1996). Several proteins (e.g., RpoH, LpxC, and SoxS) have been shown to be degraded by multiple proteases, demonstrating remarkable redundancy (Biernacka et al., 2020; Griffith et al., 2004; Kanemori et al., 1997). On a proteome-wide scale, it is unclear which proteases degrade which substrates and to what extent those substrates might overlap.

In most biological systems, protein degradation is balanced by the synthesis of new protein, making measurements of degradation rates challenging. An easy way to overcome this complication is by using translational inhibitors like cycloheximide or chloramphenicol (Belle et al., 2006; Biran et al., 2000; Li et al., 2021). Assuming that the addition of the drug does not perturb the cells aside from blocking the translation of new proteins, protein degradation can be conveniently measured by assaying changes in protein abundances over time via western blots or quantitative proteomics. However, when we performed such experiments in *E. coli,* we found that many proteins that seemed to be rapidly degraded were periplasmic (Fig. S1). Further investigation revealed that these periplasmic proteins were not degraded, but rather the addition of chloramphenicol led to the accumulation of periplasmic proteins in the bacterial growth medium (Fig. S1). Presumably, this was due to protein leakage through the outer membrane. We concluded that translation inhibitor experiments in *E. coli* could lead to major perturbations and interpreting such studies might be challenging.

A classic method to measure the unperturbed turnover of biological molecules is using radioactive isotope tracking or the combination of heavy isotope labeling and quantitative mass spectrometry (Arias et al., 1969; Foster et al., 1939). Isotopic labels can be introduced with heavy nutrients (e.g., ammonia, glucose, or amino acids) or by incubation in heavy water. Heavy ammonia, glucose, and water are comparatively cheap but result in overly complex MS1 spectra, which are difficult to interpret, particularly for lower abundance proteins (Cargile et al., 2004; Helbig et al., 2011; O'Brien et al., 2020). Most proteomic turnover studies have been performed with heavy amino acid labeling (dynamic SILAC) (Boisvert et al., 2012; Schwanhausser et al., 2011), but the small number of labeled residues limits sensitivity for short-time SILAC labeling, and missing values can hinder the coverage of multiple time points in complex systems. A further advance has been the combination of SILAC experiments and isobaric tag labeling (Savitski et al., 2018). However, these measurements tend to suffer from the inherent ratio compression of multiplexed proteomics (Pappireddi et al., 2019; Ting et al., 2011; Wenger et al., 2011). For a more detailed discussion of the advantages and limitations of various global protein turnover measurement techniques, please see the recent review by Ross et al., particularly Table S1 (Ross et al., 2021). Despite the central role of protein degradation in nearly every aspect of biological regulation, reliable and large-scale measurements are still scarce. Even fewer studies have compared degradation rates between multiple conditions (Christiano et al., 2020; Rao et al., 2008).

Here, we measure protein turnover in *E. coli* by combining heavy isotope labeling via ^{15}N ammonia with the accurate multiplexed proteomics method TMTproC (Johnson et al., 2021). We provide a rich resource of protein degradation rates for ~3.2k *E. coli* proteins (77% of all proteins in *E. coli*) measured across 12 different growth conditions with replicates. We find that active degradation rates typically are constant irrespective of changing cell division rates. When comparing degradation rates among various nutrient limitations, we find that *E. coli* recycles its cytoplasmic proteins when nitrogen-limited, and we assign substrates to proteases by measuring the change of protein turnover in knockout strains.

Results

Combining heavy isotope labeling with complement reporter ion quantification enables high-quality measurements of protein turnover.

We wanted to measure protein degradation rates and evaluate how these rates vary across growth conditions. To simplify our measurements, we grow *E. coli* in chemostats, where we can control the cell doubling time and enforce steady state (Fig. 1A). After cells reach steady state, we change the medium from unlabeled nutrients to ^{15}N-labeled ammonia. Over time, the ^{15}N-ammonia concentration in the medium increases, and newly synthesized proteins incorporate more heavy isotopes. We used ^{15}N-ammonia rather than labeled amino acids because of the higher signal we obtain with a low labeling fraction. For example, when 10% of the nutrient pool is labeled: If using heavy arginine, 90% of newly synthesized tryptic peptides ending in arginine are unlabeled. In contrast, when using heavy ammonia, a peptide having 15 nitrogens, only $(90\%)^{15}$=21% will be unlabeled. Over time the isotopic envelope of peptides will shift towards heavier forms (Fig. 1B). With the knowledge of a peptide's chemical composition and the fraction of heavy isotopes over time, we can calculate the degradation rate of the corresponding protein. However, in practice obtaining such measurements of isotopic envelopes in the MS1 spectrum is quite challenging, particularly at later time points when all the isotopic envelopes spread out and overlap with others. Additionally, missing values between measurements of various time points are a severe limitation of such approaches (O'Brien *et al.*, 2020). To overcome these limitations, we labeled each of the acquired eight time-points with TMTpro isobaric tags and combined them for co-injection into the mass spectrometer (Johnson *et al.*, 2021; Thompson et al., 2019). Analyzing these extremely complex samples with standard low m/z reporter ion quantification would lead to severe ratio distortion and measurement artifacts (Ow et al., 2009; Pappireddi *et al.*, 2019; Ting *et al.*, 2011). We overcame this limitation by programming the instrument to isolate the pseudo-monoisotopic peak (M0) and quantify the complement reporter ions in the MS2 (Fig. 1C). Figure 1D shows quantification for peptides from the expected stable protein OmpF and the expected degrading protein RpoS from carbon-limited chemostats with 6h doubling times (Schweder *et al.*, 1996). Proteins without active degradation are expected to follow the theoretical dilution curve (dotted curve) based on the chemostat dilution rate. Fitting the measured signal of OmpF peptides with a model for the expected decay of the M0 peak (solid curve) results in a turnover half-life similar to this expected value. In contrast, the fit and deduced half-life for RpoS is much shorter than the cell doubling time. We obtain half-lives for ~2.6k *E. coli* proteins with a median standard deviation of 0.3 h (Fig. 1E, Table S1). Having established this technology, we acquired similar measurements for 12 different growth conditions, each with two biological replicates (Table 1, Table S1). We then used this resource to investigate how *E. coli* adapts protein turnover under various growth conditions.

Active protein degradation rates typically do not scale with division rates.

With a method to measure protein degradation among various conditions, we determined how protein degradation scales with cell cycle time. The total turnover rate (k_{total}) is a combination of active degradation (k_{active}) and dilution ($k_{dilution}$) due to cell division (Fig. 2A). We consider two simple and reasonable models of the relationship between these two parameters. In the first model, k_{active} scales with $k_{dilution}$, i.e., the protein half-life remains a constant fraction of the cell cycle time. In the second model, active degradation rates are independent of growth rate, i.e., the active degradation rate of each protein remains constant regardless of cell doubling time. The two models have distinct predictions on how the total protein replacement half-time ($T_{1/2,}$

$_{total}$) should scale with changing cell cycle times. In the scaled model, $T_{1/2, total}$ for each protein linearly increases with cell cycle time (Fig. 2B). In contrast, in the constant model, the dilution rate dominates for rapidly dividing cells while the contribution from active degradation becomes more relevant for slower dividing cells. To test the models' predictions, we grew *E. coli* cells with a range of doubling times, including rapidly doubling cells with unlimited growth in minimal medium (0.7h) and slower doubling cells in carbon-limited chemostats (3h, 6h, and 12h). We asked how $T_{1/2, total}$ changes among these conditions (Fig. 2C). The likelihood-ratio test clearly favors the constant model regardless of which cell-cycle times we compare. This indicates that active protein degradation rates typically remain constant regardless of cell division rates. However, while we are confident that this model describes most of the proteome well, we noted interesting exceptions, particularly when comparing slower-growing cells in the chemostat to cells growing without nutrient limitation. For example, RpoS degrades faster in unlimited growth condition than the non-scaled model would predict based on chemostat measurements. This is consistent with the previous finding that RpoS is rapidly degraded in exponentially growing cells but becomes stabilized when nutrient-limited (Zhou and Gottesman, 1998). Because k_{active} rates are generally constant across cell division rates, we can more accurately measure k_{active} when $k_{dilution}$ is small. For the remainder of this study, we will focus on measurements with 6h doubling times. These conditions are experimentally easy to access, provide good resolution for active degradation, and can be extrapolated to other conditions using our insight into the constant scaling of active degradation rates.

Escherichia coli recycles its cytoplasmic proteins under nitrogen-limitation.

Next, we wanted to compare protein degradation rates under various nutrient limitations. We compared carbon (C-lim), phosphorus (P-lim), and nitrogen (N-lim) limitation measurements from chemostats with 6h doubling times. A histogram of C-lim protein half-lives indicates that most proteins are stable with a measured total half-life close to the theoretical dilution time (Fig. 3A). Using biological replicates to identify confidently degrading proteins (Fig. 3B), we found that 15% of the proteome is actively degraded in C-lim (*p*-values < 0.05). The histogram of protein half-lives under P-lim shows a similar distribution and percentage of proteins that confidently degrade as in C-lim. However, the N-lim measurements indicate that many proteins shift from stable to slowly degrading (Fig. 3A). Consistent with this, the number of confidently degrading proteins increases to 43% (Fig. 3B, *p*-value < 0.05). We found that the proteins' subcellular localization is a major predictor of the differential half-lives between N-lim vs C-lim or P-lim (Fig. 3C, D). Histograms and scatter plots of half-lives for the proteins partitioned by subcellular localization indicate that the mode for membrane and periplasmic proteins in all three conditions is very close to the theoretical dilution limit. In contrast, the mode of half-lives for cytoplasmic proteins is similar to the dilution half-life in C-lim and P-lim but is significantly shorter under N-lim, indicating that most of the cytoplasm is actively degrading under N-lim. It is difficult to confidently identify active degradation for the proteins with half-lives close to the dilution half-life. Therefore, our estimates of 43% (containing 56% of cytoplasmic, 13% of membrane, and 4% of periplasmic proteins) of the proteome actively degrading in N-lim is a very conservative estimate.

We then tested whether our finding of cytoplasmic recycling under N-lim chemostats extends to the more physiologically relevant case of batch starvation. We grew *E. coli* cells in minimal medium and switched the exponentially growing cells into medium depleted of nitrogen (Fig. 3D). Once again under nitrogen starvation, cytoplasmic proteins are degraded, and membrane/periplasmic proteins are stable. Thus, we find that *E. coli* cells slowly degrade their cytoplasmic proteins when nitrogen is scarce in both chemostats and batch culture. About 2/3 of

the cell's nitrogen is stored in proteins (Milo and Phillips, 2016). The slow degradation of proteins upon nitrogen starvation likely allows the regeneration and recycling of scarce amino acids and enables *E. coli* to produce new proteins to adapt to new environments.

Measuring protein turnover in knockout mutants allows the identification of protease substrates.

Next, we wanted to investigate protease-substrate relationships on a proteome-wide level. We were particularly interested in discovering the protease(s) responsible for the large-scale turnover of cytoplasmic proteins in N-lim. Since unfolding and degrading stably folded cytoplasmic proteins requires energy, we focused on assigning substrates to the ATP-dependent proteases. In *E. coli,* there are four known ATP-dependent protease complexes: ClpP (in complex with ClpX or ClpA), Lon, HslV (in complex with HslU), and FtsH (Mahmoud and Chien, 2018). We can identify putative substrates for these proteases by comparing the protein half-lives in protease knockout (KO) with wild-type (WT) cells (Fig. 4A). For example, the unfoldase ClpA is completely stabilized on knocking out *clpP*. ClpA's C-terminus has previously been shown to be a signal for degradation by ClpP (Maglica et al., 2008). Similarly, Tag and UhpA are identified as the substrates of Lon and HslV because their half-lives confidently increase upon knocking out the respective proteases. However, many proteins still degrade in the three protease KO lines, e.g., the phosphatase YbhA required in Vitamin B6 homeostasis still rapidly turns over with a half-life of ~1 h in each knockout strain (Sugimoto et al., 2018). Surprisingly, even the proteins that increase their half-lives in single KOs often do not get completely stabilized. Additionally, bulk cytoplasmic proteins are still degraded in all three single KOs.

Deleting *ftsH* is more complicated than the other protease genes. One of its substrates, LpxC, catalyzes the committed step in the lipid A synthesis pathway. Lipid A is the hydrophobic anchor of lipopolysaccharides (LPS), a key outer membrane component. Deletion of *ftsH* leads to increased levels of LpxC, causing an accumulation of LPS, making the cells nonviable (Ogura et al., 1999). *ftsH* null mutant cells can be rescued with a mutation of FabZ (L85P), which slows LPS synthesis and compensates for the increased LpxC levels (Ogura *et al.*, 1999). These Δ*ftsH fabZ (L85P)* cells are viable, though unfortunately they grow too slowly on minimal media and are washed out of the chemostat. We therefore could not measure protein turnover in a *ftsH* mutant similar to the other proteases. Rather, we repeated the batch nitrogen starvation experiments (Fig. 3E). Similar to the WT cells, cells lacking *ftsH* degrade cytoplasmic proteins. In contrast, membrane proteins are mostly stable (Fig. 4B). This indicates that none of the four known ATP-dependent proteases in *E. coli* are individually responsible for the large-scale cytoplasmic recycling under nitrogen scarcity.

We then asked if proteases might act redundantly, i.e., multiple proteases share a substrate, which could mask the effects of deleting individual proteases. To this end, we measured protein turnover in a triple KO line (Δ*hslV* Δ*lon* Δ*clpP*). We observe that many more proteins get stabilized in the triple KO than in any individual KO line (Fig. 4C). Strikingly, YbhA is almost completely stabilized in the triple KO, indicating that at least two of these proteases act redundantly. Nevertheless, many proteins still degrade even in the triple KO. LexA, a SOS repressor, cleaves itself under stress and unperturbed growth (Jones and Uphoff, 2021; Little, 1991). Consistent with this, LexA is still degrading in the triple KO. YoaC, an uncharacterized protein, is the shortest-lived protein in the triple knockout with a half-life of 1.2 h. It will be interesting to investigate if YoaC and many other proteins with short half-lives in the triple KO

are auto-degrading, degraded by FtsH, or if other mechanisms are at play. Furthermore, we find that the bulk of cytoplasmic proteins is slowly degraded in the triple KO under nitrogen limitation.

A quantitative comparison of protein degradation rates between the triple KO and the individual KOs allows us to assign the contribution of each protease in turning over a substrate (Fig. 4D). We can classify the substrates into six groups: those being degraded predominantly by an individual protease, those where the effects of the individual proteases are additive, those that are stabilized more in the triple KO than the combined effect of individual KOs, and those that are still actively degraded in the triple KO. We identified 64 and 14 substrates to be predominantly degraded by ClpP and Lon, respectively. We only assigned one substrate to HslV: UhpA, a transcriptional regulator that activates the transcription of genes involved in transporting phosphorylated sugars (Weston and Kadner, 1988). 81 proteins are degraded additively, a notable example of which is IbpA, a small chaperone. Previous studies have proposed that Lon either degrades free Ibps or both Ibps and bound client proteins (Bissonnette et al., 2010). We find that both ClpP and Lon contribute approximately equally to the degradation of IbpA, and their contribution is additive. We classify 59 proteins as degraded redundantly. Interestingly, 72 proteins are still confidently degraded in the triple-protease-KO line (Fig. 4E).

To validate our classifications, we compared our protease-substrate relationships with previous proteome-wide measurements. We see a large overlap (p-value = 6E-9) of our identified ClpP substrates when compared with the previous annotation of substrates via trap mutants (Fig. 4F)(Feng et al., 2013). However, we do not observe an overlap of our putative Lon-substrates with a previous Lon-trap experiment (p-value = 0.22) (Arends *et al.*, 2018). This lack of overlap is most likely caused by separating the Lon trap substrates into the different classifications, indicated by a larger overlap with the substrates from all the categories combined (p-value = 0.05). Interestingly, the putative substrates of HslV identified through a microarray study show a strong overlap with the proteins we classify as additive or redundant (p-value = 0.002) (Tsai *et al.*, 2017). This is consistent with the previous reports that HslV substrates are shared with other proteases (Kanemori *et al.*, 1997; Seong et al., 1999). We also find mild enrichment (p-value = 0.08) between substrates identified in a previous FtsH trap (Arends et al., 2016) study and additive or redundant substrates, consistent with findings that FtsH often degrades proteins that are also substrates for other proteases (Biernacka *et al.*, 2020). The lack of overlap between the proteins still degrading in the triple KO and FtsH trap substrates implies that FtsH is likely not involved in the degradation of these substrates.

Surprisingly, 40% of the active protein degradation in WT remains upon knocking out the three canonical ATP-dependent cytoplasmic proteases (Fig. 4G). We could not generate a viable quadruple KO with *ftsH* deletion, so we cannot completely rule out the possibility that all four proteases act redundantly as an explanation of the remaining protein degradation. However, the results from the individual *ftsH* knockout (Fig. 4B) and the lack of overlap between degrading proteins and the FtsH-trap experiment (Fig. 4F) are evidence against FtsH being responsible for the remaining degradation. Regardless, a major pathway for degrading proteins in *E. coli* remains to be discovered: either FtsH has a much bigger role to play than is currently believed, or a completely new mechanism degrades cytoplasmic proteins under nitrogen starvation.

Discussion

This paper introduces a technique for the global measurement of protein turnover on a gene-by-gene basis by combining complement reporter ion quantification with heavy isotope-labeled nutrients (Fig. 1). When we compare protein turnover across *E. coli* growth rates, we find that active protein degradation remains constant (Fig. 2). Based on this finding, the relative contribution of active degradation compared to dilution due to cell division must change as a function of growth rate. Therefore, relative protein levels of actively degrading proteins must change with differing cell growth rates, or cells must compensate by adjusting transcription and/or translation rates. Protein expression regulation combines gene-specific effects with such global parameters changes (Klumpp *et al.*, 2009). Our insight will help to improve genome-wide protein abundance regulation models and could help to better engineer gene expression circuits with desired properties.

Applying our method to measure protein turnover across multiple nutrient limitations, we find that most cytoplasmic proteins slowly degrade in nitrogen-limited conditions (Fig. 3). However, in phosphorus-limited and carbon-limited conditions, proteins are mostly stable. We observe this phenomenon in both a nitrogen-limited chemostat and in nitrogen-starved batch culture. The slow degradation of cytoplasmic proteins is likely a strategy *E. coli* has developed to keep scarce amino acids available, which could be critical to various metabolomic processes, including the ability to synthesize new proteins and adapt the proteome to changing environments. Bulk protein turnover measurements in the 1950s showed that *Saccharomyces cerevisiae* also increases overall protein turnover when starved of nitrogen (Halvorson, 1958), suggesting that a similar strategy might apply even to eukaryotes.

We could assign protein substrates to proteases by measuring the change in protein turnover rates of protease knockout strains (Fig. 4). We were surprised by how little protein degradation changed in the knockout strains, particularly when deleting the canonical proteases ClpP and Lon. We show that in these knockout strains, only a few proteins have a lower degradation rate, and the observed degradation of cytoplasmic proteins continues. Even when we knocked out *clpP*, *lon*, and *hslV* simultaneously, 40% of total protein turnover remains, including the cytoplasmic recycling and the degradation of many short-lived proteins. However, we observe remarkable additive and redundant effects when comparing protein turnover rates in the individual knockouts with the triple knockout. This suggests that many proteins are substrates for more than one protease. We could not extend these approaches to identify substrates for FtsH, as its deletion is lethal due to the accumulation of LPS. However, when combined with a *fabZ* mutation (Ogura *et al.*, 1999), we could show that the degradation in nitrogen-starved batch culture continues when *ftsH* is deleted. So far, we have not been able to generate viable quadruple knockout cells for all four known ATP-dependent proteases in *E. coli*. We, therefore, cannot completely rule out that FtsH is responsible for the remaining cytoplasmic degradation when the other three proteases are deleted. Regardless, a major protein degradation pathway in *E. coli* still needs to be discovered: either FtsH plays a much bigger role than generally anticipated, or there is a completely different pathway outside the four known ATP-dependent proteases. While protein degradation itself is energetically favorable, unfolding a protein requires energy. *E. coli* encodes many non-ATP-dependent proteases (Rawlings et al., 2016), but the rapidly turning over proteins in the triple knockout line and the fact that most cytoplasmic proteins are structured, suggest that some ATP-dependent unfoldase is involved. Perhaps, an adapter like ClpX or a chaperone unfolds proteins and allows those substrates to be degraded by one of the proteases that are believed to be energy independent (Rawlings *et al.*, 2016).

The discoveries in this manuscript have been enabled by introducing a new method to measure protein turnover. We chose to use heavy ammonia and glucose to label newly synthesized proteins to avoid the use of mutants and to boost the signal for short labeling times. The resulting MS1 and MS2 spectra are extremely complex, making standard quantification approaches challenging (O'Brien *et al.*, 2020). We have overcome these challenges by taking advantage of the exquisite ability of the complement reporter ion strategy (TMTproC) to distinguish real signals from the chemical background (Johnson *et al.*, 2021). The introduced methods are applicable widely beyond *E. coli*. Our ability to use comparatively cheap heavy isotope labels opens up the possibility of performing similar studies on larger animals e.g., after D_2O intake, which would be cost-prohibitive with heavy amino acid labeling (O'Brien *et al.*, 2020; Sadygov, 2021). Unlike many other cutting-edge multiplexed proteomics approaches, the applied technology is compatible with comparatively simple and widely distributed instrumentation such as quadrupole-Orbitrap instruments, as we avoid the need for an additional gas-phase isolation step. The required analysis software is available on our lab's GitHub site (https://github.com/wuhrlab/TMTProC).

We have generated a broad resource of protein turnover rates in 12 different growth conditions, each with biological replicates. The investigated conditions include varying cell cycle times from 40 minutes to 12 hours, nitrogen-, carbon-, phosphorus-limitation, and various protease knockout strains. We expect this resource to allow researchers to complement their datasets with protein turnover information. Our measurements of how protein turnover rates change in protease knockout strains will help refine protease substrate relationships. Unlike studies relying on trap experiments or protein microarrays, we could start to deduce the redundant nature of these connections. We have shown the power of the provided resource by showing cytoplasmic recycling in nitrogen-limitation and by finding a scaling law for active protein degradation rates with varying cell cycle times. Thus, we advance protein turnover measurement technology, provide a resource for ~3.2k *E. coli* protein half-lives under various conditions, and provide fundamental insight into global protein expression regulation strategies.

Acknowledgements

We would like to thank Markus Basan for the gift of triple-protease knockout strain. We thank Michaela Eickhoff, Yihui Shen, Josh Rabinowitz, Joanthon O'Brien, Joe Sheehan, Irina Mikheyeva-Bridges for advice and discussions. This work was supported by NIH grants R35GM128813 (MW), R35GM118024 (TJS), and grant T32-GM007388 (to Princeton University [EMH]), the U.S. Department of Energy, Office of Science, Office of Biological and Environmental Research under award number DE-SC0018420 and DOE grant DE-SC0018260. This work was supported in part by the National Science Foundation, through the Center for the Physics of Biological Function (PHY-1734030 [NSW]) We gratefully acknowledge support by the American Heart Association predoctoral fellowship 20PRE35220061 (TN), Princeton Catalysis Initiative (MW), Eric and Wendy Schmidt Transformative Technology Fund (MW), Harold W. Dodds Fellowship (MG), NSF Graduate Research Fellowship (ERC), Princeton University's Summer Undergraduate Research Program (EC).

Figures

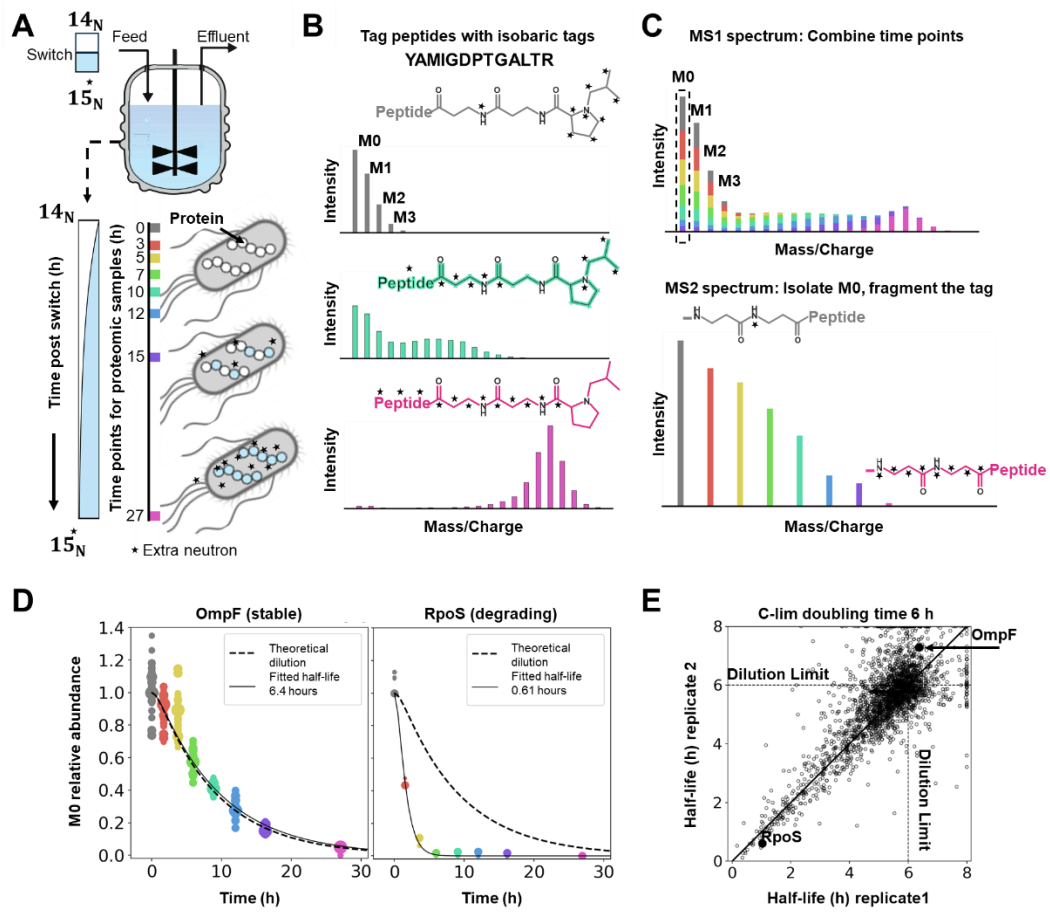

Figure 1: Combining heavy isotope labeling with an accurate multiplexed proteomics method (TMTproC) enables high-quality measurements of unperturbed protein turnover. **A)** Experimental setup. *E. coli* cells were grown in chemostats with a defined doubling time. After reaching steady state, the chemostat feed was switched to a medium with ^{15}N-labeled ammonia. Newly synthesized proteins will increasingly incorporate heavy isotopes. Proteomics samples were collected at various time points to determine the protein turnover rate. **B)** Theoretical isotopic envelopes of an example tryptic peptide, which is assumed to be stable (protein is removed from the vessel only through dilution). Over time, the increasing fraction of heavy ammonia in the peptide's structure shifts the isotopic envelope to higher masses. Peptides were labeled with isobaric tags (TMTpro) to encode different time points. **C)** Top: theoretical MS1 spectrum for a single peptide species after combining labeled peptides from all the time points. The mass spectrometer was set to isolate the monoisotopic peak (M0) and fragment the peptide. Bottom: the resulting complement reporter ions (peptide plus broken tag) enable accurate quantification of the relative abundance of the M0 over time. **D)** Example measurements for the stable OmpF protein and rapidly degrading RpoS protein. Each dot indicates the relative peptide quantification at a particular time. The size of each point is proportional to the number of measured ions. Fitting the observed data with the theoretical decay profile for M0, we can extract the half-life for each protein (solid curve). The dotted curve shows the theoretical decay for a stable protein. **E)** Scatter plot of measured protein half-lives for biological replicates of carbon-limited *E. coli* grown with a six-hour doubling time. Dotted lines indicate the cell doubling times. The solid line marks the 1:1 line. The half-lives for each

protein were calculated from the fits shown in D. Median standard deviation for the half-lives between the replicates is 0.3h.

	Strain NCM3722	Condition	Reactor type	Doubling Time	Replicates	# of proteins
1.	Wild Type	Minimal media	Batch	42 mins	2	2555
2.	Wild Type	C-lim	Chemostat	3 h	2	2665
3.	Wild Type	C-lim	Chemostat	6 h	2	2651
4.	Wild Type	C-lim	Chemostat	12 h	2	2697
5.	Wild Type	P-lim	Chemostat	6 h	2	2469
6.	Wild Type	P-lim	Chemostat	12 h	2	2619
7.	Wild Type	N-lim	Chemostat	6 h	2	2467
8.	Wild Type	N-lim	Chemostat	12 h	2	2460
9.	Δ hslV	N-lim	Chemostat	6 h	2	2393
10.	Δ lon	N-lim	Chemostat	6 h	2	2390
11.	Δ clpP	N-lim	Chemostat	6 h	2	2491
12.	Δ hslV Δ lon Δ clpP	N-lim	Chemostat	6 h	2	2809
					Union	**3252**

Table 1: Summary of the 12 growth conditions for which we measured protein turnover rates.

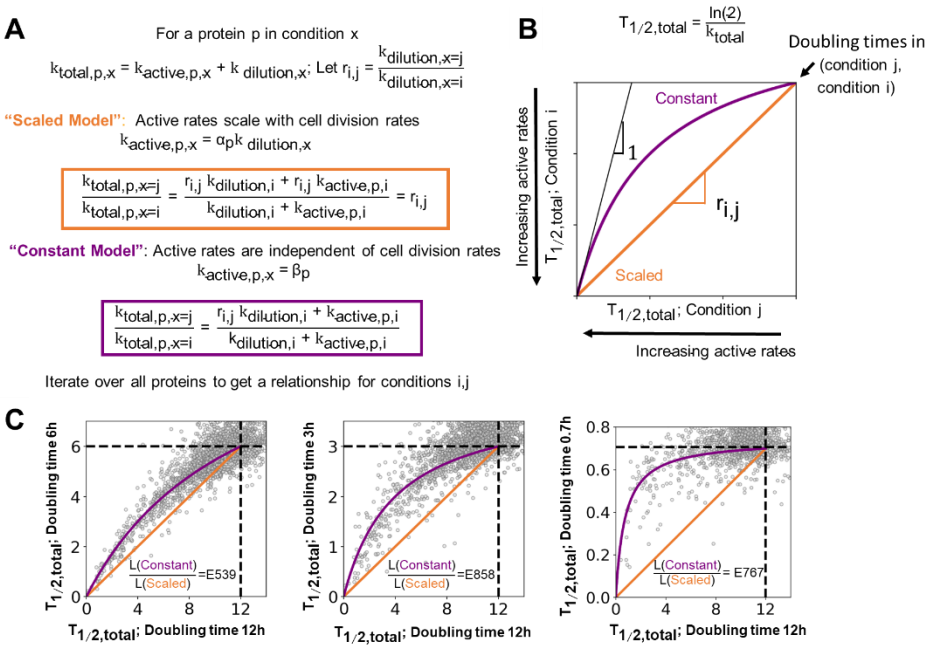

Figure 2: Active degradation rates are generally independent of cell division rates. A) Two hypothesized models describing the relationship between cell division rates and protein-specific turnover rates. The total protein turnover rate (k_{total}) is the sum of the active degradation rate (k_{active}) and the dilution rate due to cell division ($k_{dilution}$). In the "scaled model," active degradation rates increase in proportion to division rates with a protein-specific proportionality constant (α_p), i.e., active degradation remains a constant fraction of the total protein turnover rate. In the "constant model," protein-specific active degradation rates are constant (β_p), regardless of changing division rates. In this case, for slower dividing cells the contribution of active degradation becomes greater relative to dilution. **B)** $T_{1/2,\,total}$ is the time taken to replace half the protein. Theoretical plot of $T_{1/2,\,total}$ from two conditions (i, j) where cell division rates change by a factor of r. In the scaled model, $T_{1/2,\,total}$ for all the proteins lie on a straight line with slope r (orange). In the constant model, the $T_{1/2,\,total}$ follows a nonlinear relationship between the two doubling times (purple). For proteins with very high active degradation rates, the constant model predicts that $T_{1/2,\,total}$ will approach the same value for both doubling times, indicated by the slope 1 line (black). For diluting proteins with no active degradation, both models converge to the doubling times of conditions i and j. **C)** Scatter plots of protein $T_{1/2,\,total}$s for *E. coli* grown at doubling times of 42 mins (defined minimal media batch), 3 hours (C-lim), and 6 hours (C-lim) compared to 12 hours (C-lim). The dotted lines represent the dilution limit. We observe a strong statistical preference for the model in which active degradation rates are uncoupled from cell cycle duration. Shown are the likelihood ratios (L) of the constant models compared to the scaled models assuming normally distributed errors.

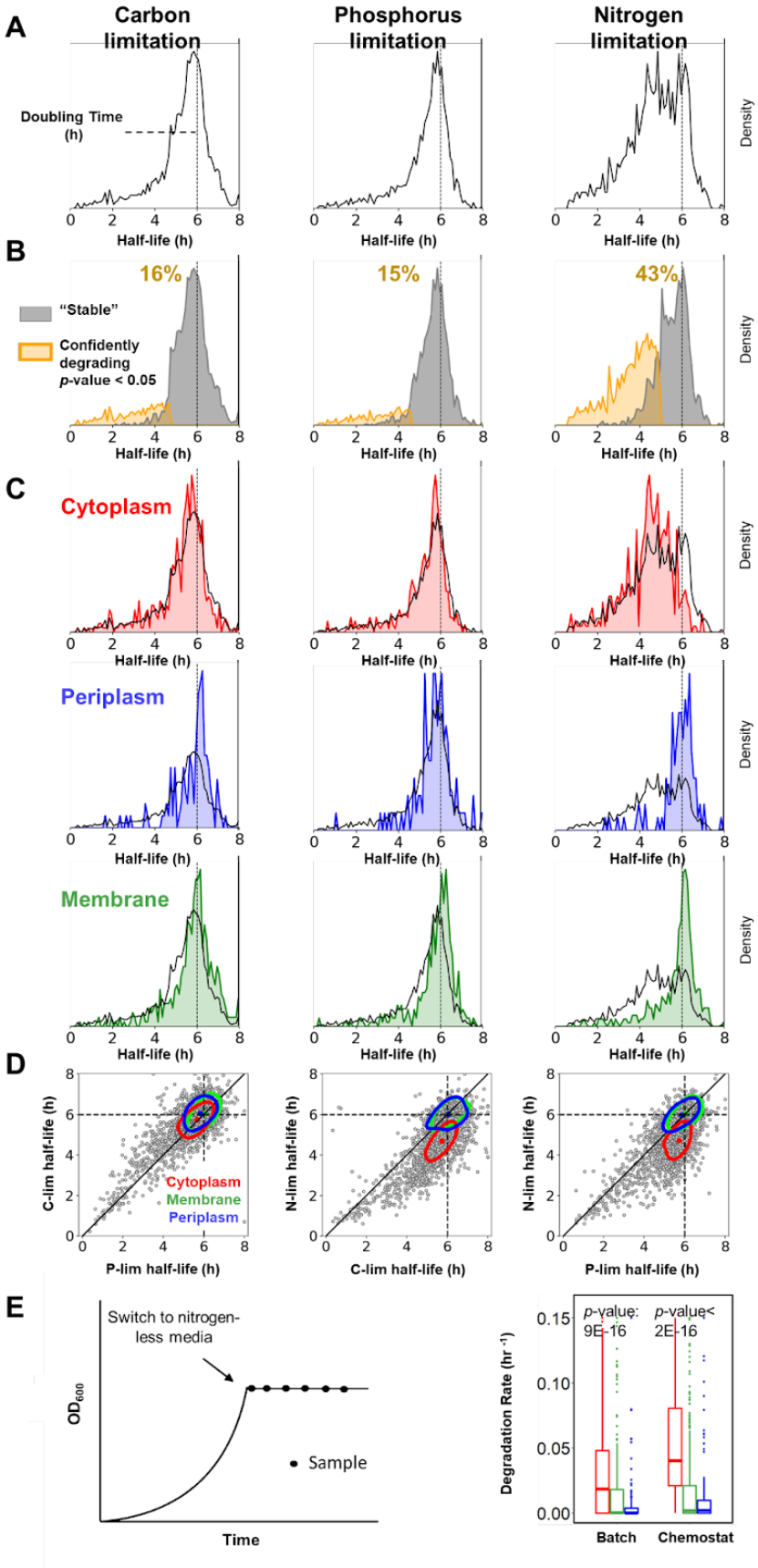

Figure 3: *E. coli* recycles its cytoplasmic proteins when nitrogen is limited. A) Histogram of protein half-lives for *E. coli* grown in chemostats under carbon (C-lim), phosphorus (P-lim), and nitrogen (N-lim) limitation. The vertical line marks the dilution limit set by the 6h doubling time. Half-lives greater than doubling time indicate measurement noise. Under C-lim and P-lim, most proteins have half-lives equal to the doubling time, suggesting they are stable. However, under N-lim, many proteins are actively degraded. **B)** Separation of the proteome into stable proteins (grey) and actively degrading proteins (yellow) (t-test, *p*-value < 0.05, n=2). In C-lim and P-lim, ~15% of the proteome turns over confidently. In contrast, under N-lim, ~ 43% of the proteome turns over. **C)** Distribution of half-lives for proteins from different subcellular localizations overlayed against the entire proteome**.** Most proteins are stable under C-lim and P-lim, irrespective of localization. However, nearly all cytoplasmic proteins slowly degrade under N-lim while the membrane and periplasmic proteomes are largely stable. **D)** Scatter plots of protein half-lives in different nutrient limitations. The dotted black lines mark the dilution limit, the solid black line denotes perfect agreement. Contour plots contain 85% of the probability mass for each subcellular compartment. The contour plots of membrane and periplasmic proteins are centered around the dilution limit in all the binary comparisons, indicating that most of these proteins are stable under all limitations. However, the shift in the contour plots of the cytoplasmic proteins on comparing N-lim with P-lim and C-lim suggests that the cytoplasmic proteins are degraded in N-lim. **E)** Measurement of protein decay rates under complete nutrient starvation in batch. Exponentially growing cells in minimal media are washed and resuspended in nitrogen-depleted media. Proteomics samples are collected after the switch and protein profiles are fitted with exponential curves to obtain the decay rates. In batch, similar to the N-lim chemostat, the cytoplasmic proteins are confidently decaying as compared to the membrane and periplasmic proteins (ANOVA).

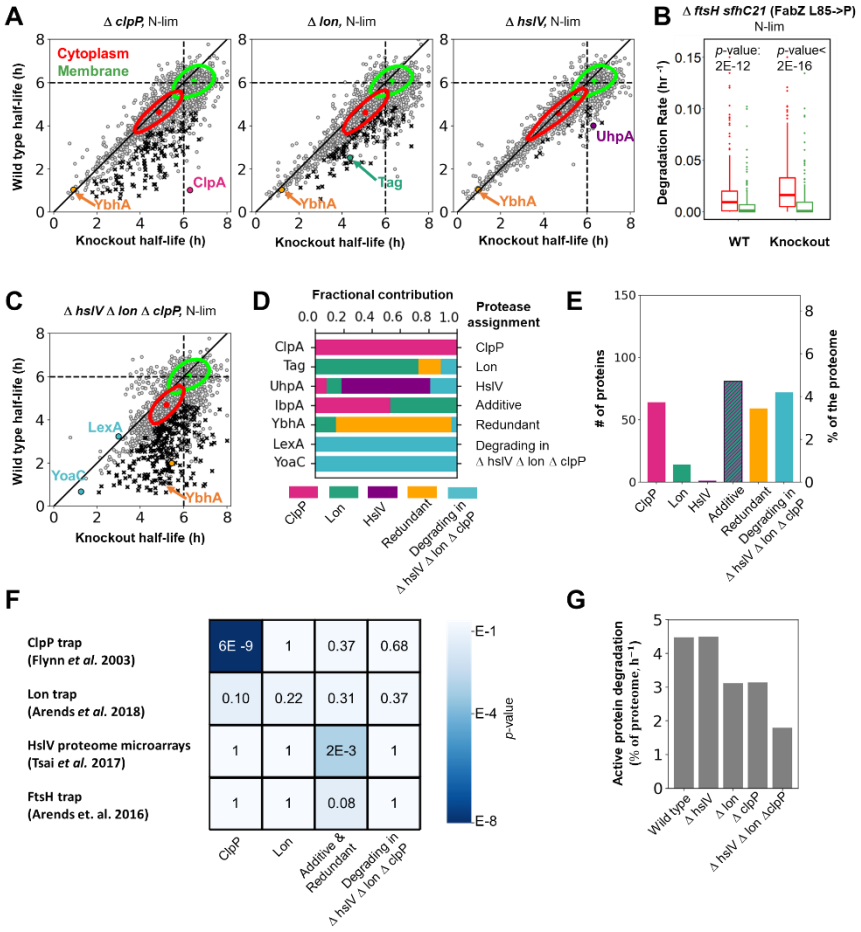

Figure 4: Measurement of protein turnover in knockout strains enables proteome-wide identification of protease substrates.

A) Scatter plots of protein half-lives of N-limited wild-type (WT) compared to Δ*clpP*, Δ*lon*, and Δ*hslV* knockout (KO) cells. Dotted lines mark the dilution limit, and the solid black line indicates perfect agreement. Substrates, marked in black, confidently increase their half-lives in KOs (t-test, *p*-value < 0.10). ClpA (in pink), tag (in teal), and UhpA (in purple) are the substrates of Δ*clpP*, Δ*lon*, and Δ*hslV,* respectively. However, the protein YbhA (in orange) is still degraded in the individual KOs. Contour plots containing 85% of the probability mass for the cytoplasmic (in red) and membrane (in green) proteins indicate that individual KOs of *hslV*, *lon*, and *clpP* retain their ability to degrade the bulk cytoplasmic proteins. **B)** Since Δ*ftsH* cells cannot grow in chemostats, we repeated the batch starvation assay as in Fig. 3E. Results indicate that the Δ*ftsH* cells, like the WT, also degrade their cytoplasmic proteins under nitrogen starvation (t-test, *p*-value = 2E-12 for WT and *p*-value < 2E-16 for Δ*ftsH*). **C)** Scatter plots of protein half-lives of WT and Δ*clpP* Δ*lon* Δ*hslV* cells in N-lim. The substrates marked in black confidently increase their half-lives in the triple KO (t-test, *p*-value < 0.10). Strikingly, many proteins are still degrading in the triple KO, e.g., LexA and YoaC in blue. In fact, the bulk cytoplasm is still turning over. However, many more proteins are stabilized in the triple KO compared to the individual KOs, indicating redundancy among substrates. E.g., YbhA, which was degrading in the individual knockouts, gets significantly stabilized in the triple KO (in orange). **D)** Comparing the shifts in the WT and KO strains' half-lives, we can assign each protease's contribution to active protein turnover. Pink, green, and purple describe the contribution of ClpP, Lon, and HslV, respectively, in stabilizing the protein. Orange marks the contribution of redundancy, defined as

the additional gain in stability upon simultaneously knocking out the three proteases as compared to the additive contributions of individual KOs. Blue represents the fraction that is unexplained by the three proteases. The bar graph represents examples from each of the six categories - turnover explained predominantly by ClpP, Lon, HslV, additive contributions, redundant contributions, and actively degrading proteins in the triple KO. **E)** Bar graph for the number of substrates and the % of the proteome assigned to each of the six categories described in D. **F)** Comparison of the substrates from our categories in E with previous proteome-wide substrate-protease assignment studies. ClpP trapped substrates significantly overlap with the identified ClpP substrates (*p*-value: 6E-9, Fisher test). Lon trapped substrates do not significantly overlap with the substrates from our categories. Previously identified substrates of HslV show a significant overlap with redundant and additive substrates. Similarly, FtsH trapped substrates significantly overlap with redundant and additive substrates in the triple KO, indicating that FtsH might also be involved in their degradation. Interestingly, however, the FtsH trapped substrates do not significantly overlap with the proteins that are still degrading in the triple KO. **G)** Comparison of the percentage of active turnover per hour across the protease KOs under N-lim. In WT cells, ~4.5% of the proteome is replaced by active degradation each hour. The proteome of Δ*hslV* cells turns over at the same rate as WT cells. Both Δ*clpP* and Δ*lon* cells had ~30% less protein turnover than WT cells. Even after knocking out *hslV*, *lon*, and *clpP* simultaneously, ~40% of the WT proteome-turnover remains, suggesting that a major pathway of protein degradation in *E. coli* remains to be discovered.

References

Alon, U. (2006). An introduction to systems biology: design principles of biological circuits (Chapman and Hall/CRC).

Arends, J., Griego, M., Thomanek, N., Lindemann, C., Kutscher, B., Meyer, H.E., and Narberhaus, F. (2018). An Integrated Proteomic Approach Uncovers Novel Substrates and Functions of the Lon Protease in Escherichia coli. Proteomics *18*, e1800080. 10.1002/pmic.201800080.

Arends, J., Thomanek, N., Kuhlmann, K., Marcus, K., and Narberhaus, F. (2016). In vivo trapping of FtsH substrates by label-free quantitative proteomics. Proteomics *16*, 3161-3172. 10.1002/pmic.201600316.

Arias, I.M., Doyle, D., and Schimke, R.T. (1969). Studies on the synthesis and degradation of proteins of the endoplasmic reticulum of rat liver. Journal of Biological Chemistry *244*, 3303-3315.

Auld, K.L., and Silver, P.A. (2006). Transcriptional regulation by the proteasome as a mechanism for cellular protein homeostasis. Cell Cycle *5*, 1503-1505. 10.4161/cc.5.14.2979.

Balakrishnan, R., Mori, M., Segota, I., Zhang, Z., Aebersold, R., Ludwig, C., and Hwa, T. (2021). Principles of gene regulation quantitatively connect DNA to RNA and proteins in bacteria. bioRxiv, 2021.2005.2024.445329. 10.1101/2021.05.24.445329.

Belle, A., Tanay, A., Bitincka, L., Shamir, R., and O'Shea, E.K. (2006). Quantification of protein half-lives in the budding yeast proteome. Proc Natl Acad Sci U S A *103*, 13004-13009. 10.1073/pnas.0605420103.

Belliveau, N.M., Chure, G., Hueschen, C.L., Garcia, H.G., Kondev, J., Fisher, D.S., Theriot, J.A., and Phillips, R. (2021). Fundamental limits on the rate of bacterial growth and their influence on proteomic composition. Cell Syst *12*, 924-944 e922. 10.1016/j.cels.2021.06.002.

Biernacka, D., Gorzelak, P., Klein, G., and Raina, S. (2020). Regulation of the First Committed Step in Lipopolysaccharide Biosynthesis Catalyzed by LpxC Requires the Essential Protein LapC (YejM) and HslVU Protease. Int J Mol Sci *21*. 10.3390/ijms21239088.

Biran, D., Gur, E., Gollan, L., and Ron, E.Z. (2000). Control of methionine biosynthesis in Escherichia coli by proteolysis. Mol Microbiol *37*, 1436-1443. 10.1046/j.1365-2958.2000.02097.x.

Bissonnette, S.A., Rivera-Rivera, I., Sauer, R.T., and Baker, T.A. (2010). The IbpA and IbpB small heat-shock proteins are substrates of the AAA+ Lon protease. Mol Microbiol *75*, 1539-1549. 10.1111/j.1365-2958.2010.07070.x.

Boisvert, F.M., Ahmad, Y., Gierlinski, M., Charriere, F., Lamont, D., Scott, M., Barton, G., and Lamond, A.I. (2012). A quantitative spatial proteomics analysis of proteome turnover in human cells. Mol Cell Proteomics *11*, M111 011429. 10.1074/mcp.M111.011429

M111.011429 [pii].

Borek, E., Ponticorvo, L., and Rittenberg, D. (1958). Protein Turnover in Micro-Organisms. Proc Natl Acad Sci U S A *44*, 369-374. 10.1073/pnas.44.5.369.

Camberg, J.L., Hoskins, J.R., and Wickner, S. (2009). ClpXP protease degrades the cytoskeletal protein, FtsZ, and modulates FtsZ polymer dynamics. Proc Natl Acad Sci U S A *106*, 10614-10619. 10.1073/pnas.0904886106.

Cargile, B.J., Bundy, J.L., Grunden, A.M., and Stephenson, J.L., Jr. (2004). Synthesis/degradation ratio mass spectrometry for measuring relative dynamic protein turnover. Anal Chem *76*, 86-97. 10.1021/ac034841a.

Christiano, R., Arlt, H., Kabatnik, S., Mejhert, N., Lai, Z.W., Farese, R.V., Jr., and Walther, T.C. (2020). A Systematic Protein Turnover Map for Decoding Protein Degradation. Cell Rep *33*, 108378. 10.1016/j.celrep.2020.108378.

Cohen-Kaplan, V., Livneh, I., Avni, N., Cohen-Rosenzweig, C., and Ciechanover, A. (2016). The ubiquitin-proteasome system and autophagy: Coordinated and independent activities. Int J Biochem Cell Biol *79*, 403-418. 10.1016/j.biocel.2016.07.019.

Erickson, D.W., Schink, S.J., Patsalo, V., Williamson, J.R., Gerland, U., and Hwa, T. (2017). A global resource allocation strategy governs growth transition kinetics of Escherichia coli. Nature *551*, 119-123. 10.1038/nature24299.

Feng, J., Michalik, S., Varming, A.N., Andersen, J.H., Albrecht, D., Jelsbak, L., Krieger, S., Ohlsen, K., Hecker, M., Gerth, U., et al. (2013). Trapping and proteomic identification of cellular substrates of the ClpP protease in Staphylococcus aureus. J Proteome Res *12*, 547-558. 10.1021/pr300394r.

Flynn, J.M., Neher, S.B., Kim, Y.I., Sauer, R.T., and Baker, T.A. (2003). Proteomic discovery of cellular substrates of the ClpXP protease reveals five classes of ClpX-recognition signals. Mol Cell *11*, 671-683. 10.1016/s1097-2765(03)00060-1.

Foster, G., Schoenheimer, R., and Rittenberg, D. (1939). The utilisation of ammonia for amino acid and ereatine formation in animals. J. Biol. Chem *127*, 319.

Griffith, K.L., Shah, I.M., and Wolf, R.E., Jr. (2004). Proteolytic degradation of Escherichia coli transcription activators SoxS and MarA as the mechanism for reversing the induction of the superoxide (SoxRS) and multiple antibiotic resistance (Mar) regulons. Mol Microbiol *51*, 1801-1816. 10.1046/j.1365-2958.2003.03952.x.

Halvorson, H. (1958). Intracellular protein and nucleic acid turnover in resting yeast cells. Biochim Biophys Acta *27*, 255-266. 10.1016/0006-3002(58)90332-9.

Helbig, A.O., Daran-Lapujade, P., van Maris, A.J., de Hulster, E.A., de Ridder, D., Pronk, J.T., Heck, A.J., and Slijper, M. (2011). The diversity of protein turnover and abundance under nitrogen-limited steady-state conditions in Saccharomyces cerevisiae. Mol Biosyst *7*, 3316-3326. 10.1039/c1mb05250k.

Jang, H.H. (2018). Regulation of Protein Degradation by Proteasomes in Cancer. J Cancer Prev *23*, 153-161. 10.15430/JCP.2018.23.4.153.

Johnson, A., Stadlmeier, M., and Wuhr, M. (2021). TMTpro Complementary Ion Quantification Increases Plexing and Sensitivity for Accurate Multiplexed Proteomics at the MS2 Level. J Proteome Res *20*, 3043-3052. 10.1021/acs.jproteome.0c00813.

Jones, E.C., and Uphoff, S. (2021). Single-molecule imaging of LexA degradation in Escherichia coli elucidates regulatory mechanisms and heterogeneity of the SOS response. Nat Microbiol *6*, 981-990. 10.1038/s41564-021-00930-y.

Kanemori, M., Nishihara, K., Yanagi, H., and Yura, T. (1997). Synergistic roles of HslVU and other ATP-dependent proteases in controlling in vivo turnover of sigma32 and abnormal proteins in Escherichia coli. J Bacteriol *179*, 7219-7225. 10.1128/jb.179.23.7219-7225.1997.

Klumpp, S., Zhang, Z., and Hwa, T. (2009). Growth rate-dependent global effects on gene expression in bacteria. Cell *139*, 1366-1375. 10.1016/j.cell.2009.12.001.

Kuroda, A., Nomura, K., Ohtomo, R., Kato, J., Ikeda, T., Takiguchi, N., Ohtake, H., and Kornberg, A. (2001). Role of inorganic polyphosphate in promoting ribosomal protein degradation by the Lon protease in E. coli. Science *293*, 705-708. 10.1126/science.1061315.

Labbadia, J., and Morimoto, R.I. (2015). The biology of proteostasis in aging and disease. Annu Rev Biochem *84*, 435-464. 10.1146/annurev-biochem-060614-033955.

Li, J., Cai, Z., Vaites, L.P., Shen, N., Mitchell, D.C., Huttlin, E.L., Paulo, J.A., Harry, B.L., and Gygi, S.P. (2021). Proteome-wide mapping of short-lived proteins in human cells. Mol Cell *81*, 4722-4735 e4725. 10.1016/j.molcel.2021.09.015.

Liang, S.-T., Bipatnath, M., Xu, Y.-C., Chen, S.-L., Dennis, P., Ehrenberg, M., and Bremer, H. (1999). Activities of constitutive promoters in Escherichia coli. Journal of molecular biology *292*, 19-37.

Liang, S.-T., Xu, Y.-C., Dennis, P., and Bremer, H. (2000). mRNA composition and control of bacterial gene expression. Journal of bacteriology *182*, 3037-3044.

Little, J.W. (1991). Mechanism of specific LexA cleavage: autodigestion and the role of RecA coprotease. Biochimie *73*, 411-421. 10.1016/0300-9084(91)90108-d.

Liu, H., Urbe, S., and Clague, M.J. (2012). Selective protein degradation in cell signalling. Semin Cell Dev Biol *23*, 509-514. 10.1016/j.semcdb.2012.01.014.
Maglica, Z., Striebel, F., and Weber-Ban, E. (2008). An intrinsic degradation tag on the ClpA C-terminus regulates the balance of ClpAP complexes with different substrate specificity. J Mol Biol *384*, 503-511. 10.1016/j.jmb.2008.09.046.
Mahmoud, S.A., and Chien, P. (2018). Regulated Proteolysis in Bacteria. Annu Rev Biochem *87*, 677-696. 10.1146/annurev-biochem-062917-012848.
Mandelstam, J. (1957). Turnover of protein in starved bacteria and its relationship to the induced synthesis of enzyme. Nature *179*, 1179-1181. 10.1038/1791179a0.
Milo, R., and Phillips, R. (2016). Cell biology by the numbers (Garland Science, Taylor & Francis Group).
Neher, S.B., Flynn, J.M., Sauer, R.T., and Baker, T.A. (2003). Latent ClpX-recognition signals ensure LexA destruction after DNA damage. Genes Dev *17*, 1084-1089. 10.1101/gad.1078003.
O'Brien, J.J., Narayan, V., Wong, Y., Seitzer, P., Sandoval, C.M., Haste, N., Smith, M., Rad, R., Gaun, A., Baker, A., et al. (2020). Precise Estimation of In Vivo Protein Turnover Rates. bioRxiv, 2020.2011.2010.377440. 10.1101/2020.11.10.377440.
Ogura, T., Inoue, K., Tatsuta, T., Suzaki, T., Karata, K., Young, K., Su, L.H., Fierke, C.A., Jackman, J.E., Raetz, C.R., et al. (1999). Balanced biosynthesis of major membrane components through regulated degradation of the committed enzyme of lipid A biosynthesis by the AAA protease FtsH (HflB) in Escherichia coli. Mol Microbiol *31*, 833-844. 10.1046/j.1365-2958.1999.01221.x.
Ow, S.Y., Salim, M., Noirel, J., Evans, C., Rehman, I., and Wright, P.C. (2009). iTRAQ underestimation in simple and complex mixtures: "the good, the bad and the ugly". J Proteome Res *8*, 5347-5355. 10.1021/pr900634c.
Pahl, H.L., and Baeuerle, P.A. (1996). Control of gene expression by proteolysis. Curr Opin Cell Biol *8*, 340-347. 10.1016/s0955-0674(96)80007-x.
Pappireddi, N., Martin, L., and Wuhr, M. (2019). A Review on Quantitative Multiplexed Proteomics. Chembiochem *20*, 1210-1224. 10.1002/cbic.201800650.
Rao, P.K., Roxas, B.A., and Li, Q. (2008). Determination of global protein turnover in stressed mycobacterium cells using hybrid-linear ion trap-fourier transform mass spectrometry. Anal Chem *80*, 396-406. 10.1021/ac701690d.
Rawlings, N.D., Barrett, A.J., and Finn, R. (2016). Twenty years of the MEROPS database of proteolytic enzymes, their substrates and inhibitors. Nucleic Acids Res *44*, D343-350. 10.1093/nar/gkv1118.
Rosenfeld, N., and Alon, U. (2003). Response delays and the structure of transcription networks. J Mol Biol *329*, 645-654. 10.1016/s0022-2836(03)00506-0.
Ross, A.B., Langer, J.D., and Jovanovic, M. (2021). Proteome Turnover in the Spotlight: Approaches, Applications, and Perspectives. Mol Cell Proteomics *20*, 100016. 10.1074/mcp.R120.002190.
Savitski, M.M., Zinn, N., Faelth-Savitski, M., Poeckel, D., Gade, S., Becher, I., Muelbaier, M., Wagner, A.J., Strohmer, K., Werner, T., et al. (2018). Multiplexed Proteome Dynamics Profiling Reveals Mechanisms Controlling Protein Homeostasis. Cell *173*, 260-274 e225. 10.1016/j.cell.2018.02.030.
Schwanhausser, B., Busse, D., Li, N., Dittmar, G., Schuchhardt, J., Wolf, J., Chen, W., and Selbach, M. (2011). Global quantification of mammalian gene expression control. Nature *473*, 337-342. 10.1038/nature10098.
Schweder, T., Lee, K.H., Lomovskaya, O., and Matin, A. (1996). Regulation of Escherichia coli starvation sigma factor (sigma s) by ClpXP protease. J Bacteriol *178*, 470-476. 10.1128/jb.178.2.470-476.1996.
Scott, M., Gunderson, C.W., Mateescu, E.M., Zhang, Z., and Hwa, T. (2010). Interdependence of cell growth and gene expression: origins and consequences. Science *330*, 1099-1102. 10.1126/science.1192588.

Sugimoto, R., Saito, N., Shimada, T., and Tanaka, K. (2018). Identification of YbhA as the pyridoxal 5'-phosphate (PLP) phosphatase in Escherichia coli: Importance of PLP homeostasis on the bacterial growth. J Gen Appl Microbiol *63*, 362-368. 10.2323/jgam.2017.02.008.

Thompson, A., Wolmer, N., Koncarevic, S., Selzer, S., Bohm, G., Legner, H., Schmid, P., Kienle, S., Penning, P., Hohle, C., et al. (2019). TMTpro: Design, Synthesis, and Initial Evaluation of a Proline-Based Isobaric 16-Plex Tandem Mass Tag Reagent Set. Anal Chem *91*, 15941-15950. 10.1021/acs.analchem.9b04474.

Ting, L., Rad, R., Gygi, S.P., and Haas, W. (2011). MS3 eliminates ratio distortion in isobaric multiplexed quantitative proteomics. Nat Methods *8*, 937-940. 10.1038/nmeth.1714.

Tsai, C.H., Ho, Y.H., Sung, T.C., Wu, W.F., and Chen, C.S. (2017). Escherichia coli Proteome Microarrays Identified the Substrates of ClpYQ Protease. Mol Cell Proteomics *16*, 113-120. 10.1074/mcp.M116.065482.

Wenger, C.D., Lee, M.V., Hebert, A.S., McAlister, G.C., Phanstiel, D.H., Westphall, M.S., and Coon, J.J. (2011). Gas-phase purification enables accurate, multiplexed proteome quantification with isobaric tagging. Nat Methods *8*, 933-935. 10.1038/nmeth.1716.

Weston, L.A., and Kadner, R.J. (1988). Role of uhp genes in expression of the Escherichia coli sugar-phosphate transport system. J Bacteriol *170*, 3375-3383. 10.1128/jb.170.8.3375-3383.1988.

Westphal, K., Langklotz, S., Thomanek, N., and Narberhaus, F. (2012). A trapping approach reveals novel substrates and physiological functions of the essential protease FtsH in Escherichia coli. J Biol Chem *287*, 42962-42971. 10.1074/jbc.M112.388470.

Wettstadt, S., and Llamas, M.A. (2020). Role of Regulated Proteolysis in the Communication of Bacteria With the Environment. Front Mol Biosci *7*, 586497. 10.3389/fmolb.2020.586497.

Zhou, Y., and Gottesman, S. (1998). Regulation of proteolysis of the stationary-phase sigma factor RpoS. J Bacteriol *180*, 1154-1158. 10.1128/JB.180.5.1154-1158.1998.